

# UNSTEADY SIMULATIONS OF ROTORCRAFTS IN GROUND EFFECT USING A FAST PANEL – FAST VORTEX FORMULATION

Alberto Verna<sup>§</sup>, Andrea D’Andrea\*

AgustaWestland Aerodynamics Dept.  
Via G. Agusta 520, 21017 Cascina Costa (VA), Italy

<sup>§</sup>Aerodynamic Specialist, E-mail: [alberto.verna@agustawestland.com](mailto:alberto.verna@agustawestland.com)

\*Rotor Aerodynamics Technical Leader, E-mail: [andrea.dandrea@agustawestland.com](mailto:andrea.dandrea@agustawestland.com)

## ABSTRACT

Since the last past years, there have been several attempts to simulate entire helicopter configurations using lifting surface (or panel) codes coupled with different free-wake vortex models. Results normally exhibit a good level of correlation at least in steady level forward flight conditions out of ground effect (OGE). However, in case of rotorcraft operations very close to the ground (IGE - in ground effect), several phenomena have still remained a challenge to be numerically simulated by rotorcraft potential tools because the strong non-linear effects induced by the ground on the development of rotor wake. At the same time, the usage of Eulerian of Navier-Stokes solvers, seem to be a strong challenge because of the enormous amount of required computational times and allocated computer memory. Experimental and numerical studies led up to now on this subject, have confirmed that as a hovering rotor moves from OGE conditions toward the ground, the wake starts to impinge on it and converts out with a strong radial component. IGE operations in forward flight complicates further more the aerodynamics environment around the helicopter. At very low advance ratios, a small region of ‘flow recirculation’ is formed upstream of the rotor, increasing the inflow through the forward part of the rotor disk. At a bit higher advance ratios, previous recirculation disappeared, and a large vortex (‘ground vortex’) occurs below the rotor making the flow more uniform. This ground vortex is finally overrun with the increasing of the helicopter advancing speed. Normally, positioning and generation of the ground vortex can happen intermittently in time further increasing flowfield unsteadiness and pilot workload in these transitional flight regimes, which occur as a strong function of advance ratio and of square root of the disk loading. Present paper will present the capability of the tool *ADPANEL* (AgustaWestland in-house developed) to simulate and predict the unsteady vortical flows generated by a rotorcraft operating on ground, both in Hover and in Forward-Flight. Different rotor configurations will be examined in present work, taking into account a change in rotor solidity and in its disk-loading value. Particular emphasis will be given to the understanding of main characteristics of different regimes occurring in IGE, as well as to the numerical assessment of velocity and vorticity unsteadiness of ground-vortex-structures dominated flows.

## 1 NOTATION

$A$	rotor disk area ( $A = \pi R^2$ )
$c$	blade chord
$C_T$	rotor thrust coefficient, thrust scaled by $\rho A (\omega R)^2$
$h$	height of the rotorcraft with respect to the ground (measured at the hub center)
$n$	number of blades
$\bar{n}$	normal unit vector (positive inboard)
$r$	rotor radial station
$\hat{r}$	vector distance
$R$	rotor radius
$S$	body surface
$T$	rotor thrust
$v$	Induced vertical velocity from momentum theory
$V$	aircraft speed
$V_{TIP}$	tip speed
$\bar{V}_\infty$	freestream velocity
$z$	vertical (normal to the ground) station
$\Gamma_v$	tip vortex circulation
$\mu$	advance ratio
$\mu^*$	normalized advance ratio $\left( \mu^* = \mu / \sqrt{C_T/2} \right)$

$\hat{\mu}$	doublets’ strength
$\rho$	air density
$\sigma, s$	rotor solidity ( $\sigma = (nc)/(\pi R)$ )
$\hat{\sigma}$	sources’ strength
$\omega$	rotor angular velocity

## 2 ABBREVIATIONS

AW	AgustaWestland
CFD	Computational Fluid Dynamics
CPU	Central Processing Unit
CVC	Constant Vorticity Contour
DPIV	Digital Particle Image Velocimetry
HIGE	Hovering In Ground Effect
HOGE	Hovering Out of Ground Effect
IGE	In Ground Effect
ISA	International Standard Atmosphere
OGE	Out of Ground Effect
RMS	Root Mean Square
SL	Sea Level

## 3 INTRODUCTION

The accurate prediction of the aerodynamic behavior of full-aircraft configurations is a challenging and significant issue for every rotorcraft manufacturer company. The unsteady aerodynamic interaction between rotating wings, their trailed wakes and fixed airframes, normally affects

rotor performances, handling qualities, acoustic emission and vibratory levels in several ways. Such a complex environment requires a huge amount of computational time and resources to be simulated with Euler or Navier-Stokes equations-based tools. Therefore, in the last decade, many efforts to simulate entire helicopter configurations using potential-based (lifting surface or panel) codes have been made, and different free-wake vortex models have been developed. These tools exhibit a good level of correlation both in hover and in level forward flight conditions out of ground effect, with much less computational efforts compared to the common CFD tools<sup>[1]-[5]</sup>. However, when operating close to the ground, several non-linear phenomena induced by the ground itself on the development of rotor wake make this topic challenging to be simulated by whatever computational tool. Numerical studies, performed up to now mainly in hovering conditions, have confirmed the experimental observations that, starting from a OGE condition and reducing the rotor height above the ground, the wake starts to impinge on it and convects out with a significant radial component. Turbulent diffusion and vortex pairing phenomena strongly affect the wake development. As a result, the rotor inflow changes and the rotor thrust usually increases for a given power or collective pitch angle. The IGE forward flight condition is even more complicated and the behavior strongly depends on the advance ratio combined with the height above the ground<sup>[11]-[14]</sup>. At very low advance ratios, the vortices move radially away from the rotor interacting with the freestream, and a region of *flow recirculation* is formed upstream of the rotor, increasing the inflow through the forward part of the disk. In contrast with the increasing of performances obtained in hover when the rotor is operating close to the ground, the effect of previous flow recirculation is to increase the induced power and requires the pilot for a significant left-stick control. Such region of recirculating flow moves towards the rotor as the advance ratio increases, and finally passes under its leading edge. The recirculation zone diameter reduces and a well defined vortex (*ground vortex*) occurs below the rotor making the flow more uniform. Unfortunately, experimental studies led up to now on this subject demonstrated that the generation and positioning of the ground vortex can happen intermittently in time depending on the advance ratio and on the disk loading, increasing again the pilot workload in this transitional flight regime. Ground vortex is finally overrun with a further increasing of the advance ratio, when pilot left-stick intervention on the opposite direction is suddenly required.

The accurate aerodynamic prediction of the flowfield around a rotorcraft operating in ground effect conditions is currently challenging the global aeromechanics helicopter community, since several authors have shown that it is strictly connected with brownout phenomenon<sup>[15]</sup>.

Aim of this paper is to extend by means of numerical computations, carried out with the AgustaWestland in-house code ADPANEL<sup>[3],[5]</sup>, the knowledge on this field. After a brief description of ADPANEL features, the capability of the code to predict the unsteady flows generated on ground in HIGE conditions is presented by means of the recent and exhaustive experimental data obtained by Leishman et al.<sup>[10]</sup>. The second part of this work deals with forward flight operations IGE, focusing on the effect of rotor solidity on the ground vortex regime

onset. For this purpose, two sets of blades with different solidity ( $\sigma=0.08$  -  $\sigma=0.12$ ) will be analyzed. Numerical results are presented under a topological point of view for such as concern the flow regimes instauration. Finally, numerical post-processing has been applied in order to identify the vortex size and positioning and highlight the flowfield unsteadiness.

## 4 NUMERICAL METHOD

The accurate prediction of the aerodynamic behavior of a rotorcraft operating on ground involves at present every helicopter manufacturer company. Due to the complex physics of the phenomena occurring in IGE, as well as because of the low frequency unsteadiness representative of rotor aerodynamics in such conditions, numerical simulations have to be carried out for long computational time in order to guarantee an acceptable level of accuracy. In this view, it has long been evident the need for a computationally efficient tool able to analyze helicopter operations in ground effect without making use of Euler or Navier-Stokes methods, based on finite difference/finite volume approach. These codes, in fact, have to face with enormous amounts of computational time and computer memory in assessing the aerodynamic environment around a rotorcraft. Although during the past years computational fluid dynamics has been used with varied success to model helicopter aerodynamics<sup>[16],[17]</sup>, significant difficulties remain in combining rotating and fixed frames, and in avoiding numerical dissipation of vorticity commonly caused by the low-order accuracy of the spatial-solver. Vorticity dissipation plays a not-marginal negative role, especially because of the necessity to simulate an enormous amount of rotor revolutions. Phillips and Brown<sup>[18]</sup> showed that almost one-hundred rotor revolutions are necessary to capture the low-frequency unsteadiness of rotor wake in ground effect. Additionally, many rotor turns have to be modeled in order to allow initial transients within CFD calculations to dissipate. However, even if CFD-based methods were demonstrated to be very effective in predicting rotor outwash, numerical computations must solve the rotor wake dynamics in computational times much less than those ones shown by such tools. Potential methods seem to be very helpful in this direction. Several works based on this approach confirmed the possibility to get good predictions of both rotor performance and induced velocities on ground, with computational times and costs that are orders of magnitude less than CFD methods<sup>[15]</sup>.

### 4.1 ADPANEL Code Description

ADPANEL<sup>[3]</sup> is a Full-Unstructured Panel code coupled with a Time-Stepping Full Span Free Wake Vortex model. This state-of-the-art tool embeds the most advanced aerodynamic features concerning potential methods, especially for the possibility to represent the bodies' surfaces with unstructured-hybrid mesh, handling with both quadrilateral and triangular cells, for a Constant Vorticity Contour (CVC) wake model available for both rotary and fixed wings, and for its Multi-Processor (MPI) implementation.

Thanks to this features ADPANEL is able to analyze in short computational times and with detailed predictions

entire helicopters and tiltrotors configurations even operating in ground effect (Figure 1). Although ADPANEL is not based on *Fast Multipole Methods*, such as those ones developed by Greengard and Rokhlin<sup>[8]-[9]</sup>, the present tool can exhibit resolution times quite less than those offered by any other standard or direct methods, thanks to a special multi-block iterative solver, a physics-based approximation of the far-field inductions, and thanks to its Multi-Processor implementation.

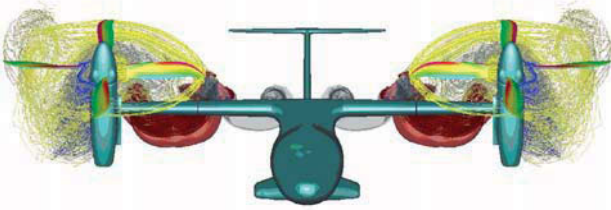


**Figure 1: ADPANEL solution and CVC wake development for a full-tiltrotor configuration operating OGE.**

### ADPANEL - Basic Formulation

Considering a body with known boundaries  $S$  submerged in a potential flow, then the laplacian of the total potential must be null (Laplace equation) to enforce incompressibility, irrotationality and mass conservation. Following the well known Green's identity<sup>[22]</sup>, the general solution to the previous equation can be constructed by a sum of *sources* and *doublers*. The zero normal flow on the body can be achieved indirectly imposing the value of the total potential on the boundary, applying the formulation known as *Dirichlet problem*. It can be demonstrated that, by setting the strength of sources  $\sigma$  from initial conditions locally proportional to the freestream velocity component normal to the surface, a much simplified set of equations for the doublers' strength  $\hat{\mu}$  (Eq. (1) and Eq. (2)) can be obtained.

$$(1) \quad \underbrace{\frac{1}{4\pi} \int_{\text{body+wake}} \left[ \hat{\mu} \bar{n} \cdot \bar{\nabla} \left( \frac{1}{r} \right) \right] dS}_{\text{Doublers}} - \underbrace{\frac{1}{4\pi} \int_{\text{body}} \left[ \hat{\sigma} \left( \frac{1}{r} \right) \right] dS}_{\text{Sources}} = 0$$

$$(2) \quad \sigma = \bar{V}_{\infty} \cdot \bar{n}$$

### ADPANEL - Advanced Direct Solver

A boundary element code based on a direct solution of the aforementioned equations is called a direct panel method. The equations are first of all discretized along the surface of the body by means of several panels. The Dirichlet boundary condition should be specified at each of these elements at specific *collocation points*. In the case of absence of wake panels, for example, Eq. (1) will assume the following form:

$$(3) \quad \sum_{k=1}^N \frac{1}{4\pi} \int_{\text{panel}-k} \left[ \hat{\mu}_k \bar{n}_k \cdot \bar{\nabla} \left( \frac{1}{r} \right) \right] dS_k + \sum_{k=1}^N \frac{1}{4\pi} \int_{\text{panel}-k} \left[ \hat{\sigma}_k \left( \frac{1}{r} \right) \right] dS_k = 0$$

where we have indicated with  $N$  the total number of panels.

Since the source strengths are known and set by initial conditions, the previous equation (that has to be written for each collocation point) represents an *algebraic linear system* containing the  $N$  unknown singularity variables  $\hat{\mu}_k$ . Once solved the above system, the unknown singularity values (doublers' strengths) are obtained. Finally, the velocity components are evaluated in terms of local coordinates on panels by using numerical differential operations along the body surface.

The described approach is the so-called direct formulation, and usually poses not negligible problems in terms of computational times and allocated memory in order to invert the system matrix. Considering  $N$  panels on the body, then the  $N \times N$  system would require computational times growing as  $O(N^3)$ . Advanced-fast panel methods, however, are able to exhibit solution times that grow as  $O(N \log N)$  (see Figure 2). The other great limitation affecting the direct resolution is the storage requirement of the matrix, that obviously grows as  $O(N^2)$  and very quickly reaches prohibitive values.

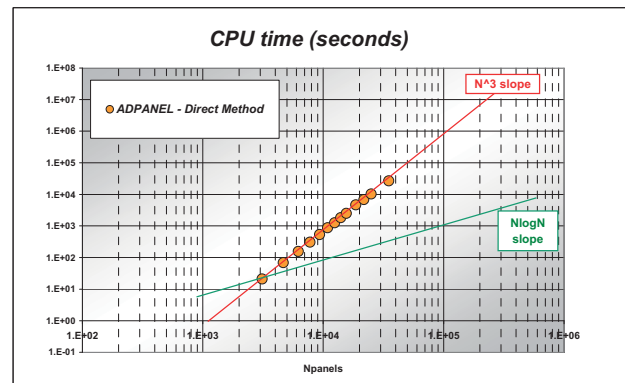


**Figure 2: CPU time requirements for a direct solution with ADPANEL (versus number of panels).**

### ADPANEL - Multi-Block Iterative Solver

In order to avoid the direct resolution of the linear system, ADPANEL computes the final potential solution by means of an iterative approach whose concept is totally based on the *linear physics* of the Laplace equation. More in detail, for every iteration in time, an *unsteady iterative process* (advancing along a "pseudo-time") is led in order to obtain the final numerical solution.

The panels in which the body surface is discretized are grouped into different *blocks* (a *block* is simply a grouping of a specific number of *near cells*) by means of a dedicated algorithm that ensures a similar number of elements inside each block. For every physical iteration in time, each block is firstly solved without taking into account the effect of the potential induced from different ones on itself. Afterwards, during the second (or successive) iteration along the pseudo-time, ADPANEL starts to solve the sets of equations for every block by adding the potential effect generated from different ones on the right side of the system, whose inductions are evaluated by using the solution computed at the previous pseudo-time. During this iterative process, a *time-variable-*

*relaxation scheme* (based on the temporary local slope of the block residual) is added to stabilize the solution. Great savings in computational time are provided by this process, especially because during the firsts pseudo-iterations the mutual effect between far-blocks is strongly approximate. Moreover, during the iterative process, several blocks reach a good convergence level before other ones, and are therefore removed from the loop. In case of real-unsteady problems, this iterative procedure restarts its solution from the previous one, with a great saving of computational time. Finally, with this iterative approach, the full-matrix representing the linear system has not to be stored. ADPANEL, indeed, needs only to store the induction coefficients of one block on itself with a direct gain in terms of memory storage requirement.

### ADPANEL - Accelerated Flow Solver

Exact integral solution for the influence coefficient calculations are necessary only when the distance between control point and the panel center is small<sup>[22]</sup>. In fact, when the distance between the evaluation point and the panel gets bigger than 4 times the maximum diagonal of the panel itself, the integral evaluation can be reduced to a point calculation. Conversely, we can expect that errors will also be small if distant panels are grouped into different *groups* and their mutual inductions evaluated by means of approximate formulae in order to accelerate the *block-to-block induction procedure*. It is worth underlining that during the iterative process previously described, potential inductions within the same block are evaluated in ADPANEL by straightly solving the full-integrals.

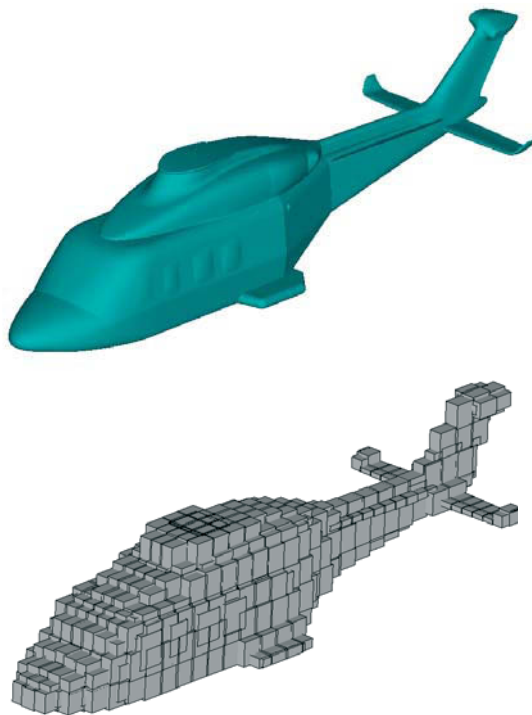


**Figure 3: example of a clean helicopter fuselage mesh (top) and its repartitions in groups (bottom)**

Obviously, whenever cell-to-cell distances become large, common reduced formulae based on point calculations are

used even within the same block. Afterwards, in order to take into account potential inductions between different blocks, mutual inductions are evaluated by means of *approximate calculations*. The procedure of cell repartition in groups is led during the iterative process described above. During this process, ADPANEL starts to generate a coarse group repartition (*low level*) and with the decreasing of residuals it goes towards a finer repartition (*high level*), so that the errors generated by the approximations may be reduced with the evolution along the pseudo-time.

The approximate procedures implemented in ADPANEL to evaluate *group-to-group* interactions are various and depend on the geometrical distance between different groups; for instance, one type of approach, quite similar to those based on *subgrid* approximations, can be summarized in the following two points:

- exact potential calculation on all vertices and centroid of the Cartesian box representing the group;
- interpolation procedure (based on inverse distance formulae) to get back the potential on all cells present inside the group.

With these two methodologies, ADPANEL is finally able to reach computational times greatly reduced with respect to those showed for the previous direct formulation. More in detail, ADPANEL requires CPU times that seem to grow as  $O(N^{4/3})$  (Figure 4).

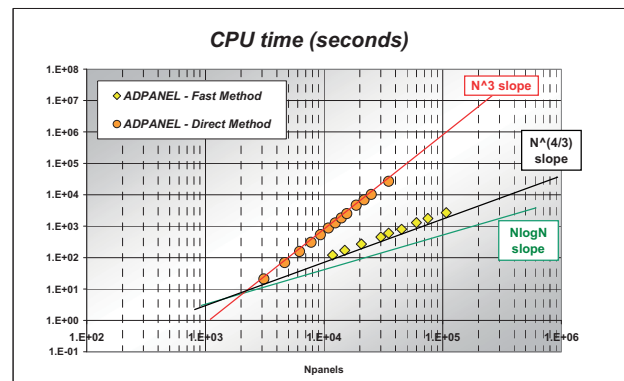


**Figure 4: comparison in terms of CPU time for a direct and fast solution with ADPANEL (versus number of panels).**

### ADPANEL - CVC Wake Model

In boundary elements methods, in order to guaranty an inviscid flow, a Kutta condition is applied at all rotating and fixed wings trailing edges.

The wake modeling implemented in ADPANEL is composed of two parts: a *dipole buffer wake sheet*, and a set of *Constant Vorticity Contour (CVC) vortex filaments*. They are deputed to represent the vorticity released from the wing for both the *trailed* and *shed* components (respectively generated by spanwise and temporal variations of the bound circulation). The buffer wake sheet is a *short dipole* (consisting in a sequence of doublets) trailing all the lifting surface and starting from its trailing edge. In the spanwise direction, the buffer wake is comprised of the same amount of panels as the wing

trailing edge. This dipole is generated every time step and is converted (after the resolution of the Laplace equation) in CVC vortex filaments. Before the conversion, starting from the second time iteration, an equivalent vortex is generated along the confinement of the buffer region in order to erase the not-balanced amount of circulation (Figure 5).

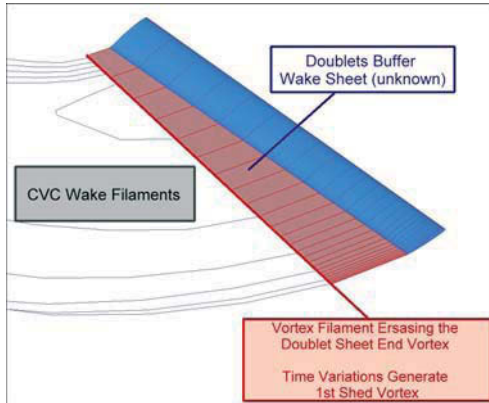


Figure 5: ADPANEL CVC wake model – doublets buffer wake sheet and CVC filaments.

The CVC wake modeling allows to generate refined roll-up and high spanwise resolution without enforcing an unnecessary large number of wake elements along the blade. ADPANEL benefits by recent and well-validated “vortex dissipation laws” for properly representing the vortex core increasing with the time passing, as well as “vortex-straining-models” such as those ones developed by Leishman et al.<sup>[6],[7]</sup>

An approximate numerical approach for evaluating velocity-inductions of CVC wake filaments on the wake itself and on the body (fast vortex formulation), is implemented in ADPANEL as specifically described in Ref. [3]. This approach is very similar to what previously shown in present work for the body cell-cell induction-process. That is, all CVC filaments are encapsulated in several boxes, and as soon as distance between different ones become large, their mutual inductions can be evaluated by generating ‘macro-vortex structures’ depending on the geometrical characteristic of the filaments within the box<sup>[3]</sup>.

We have to highlight that in case of numerical simulations of helicopters operating on ground, a CVC free-wake vortex model represents a great advantage in terms of computational times with respect to the more common vortex-lattice methods<sup>[22]</sup>.

#### 4.2 In Ground Effect Applications and Validation

In case of numerical simulations of rotorcrafts operating in ground effect, two different approaches can be used in ADPANEL. The first one is based on the usage of a three-dimensional plane representing the ground; such plane is generally built with potential doublets and sources in order to reflect the vortex filaments impinging on it. The second one is contrarily based on the application of a vortex image system. This latter approach has been adopted for all the following simulations.

The capability of ADPANEL to accurately predict both rotor performance and time-averaged velocity fields in case of rotorcraft operations in HIGE will be fully demonstrated in the course of this work, by using reliable experimental data recently obtained by Leishman et al.<sup>[10]</sup>. Thanks to extremely precise instruments, the authors were able to measure the changing of the flowfield with respect to the OGE condition for different operative heights of the rotor. However, their tests were carried out only in hovering, since the difficulty to reproduce realistic boundary conditions for forward flight applications in wind tunnel (aircraft in motion with respect to the ground). Their experiments were conducted using flow visualizations and ‘phase-resolved digital particle image velocimetry’ (DPIV) to examine the fluid dynamics of the rotor wake interacting with the ground plane.

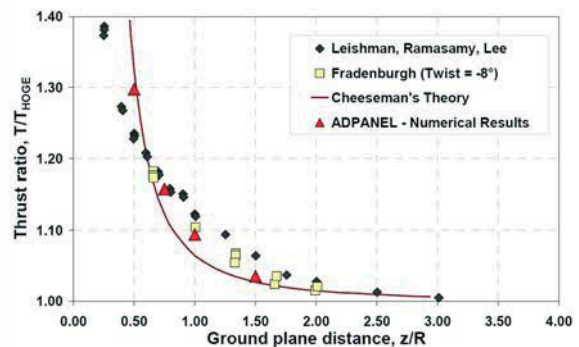


Figure 6: comparison of rotor performances between ADPANEL results and experimental measurements.

Figure 6 reports the ADPANEL numerical results with respect to the experimental data in terms of rotor thrust-level increase with respect to the OGE condition at constant required power. ADPANEL results are totally in agreement with the experimental data coming from Leishman et al., but also with wind tunnel test data and theoretical predictions coming from similar additional works (for instance, by Fradenburgh<sup>[19]-[20]</sup> and Cheeseman<sup>[21]</sup>).

The performance agreement, however, is not enough to validate a numerical tool for ground effect applications, and a detailed correlation with time-averaged velocity profiles is mandatory to be sure that wake dynamics is well reproduced.

Taking into account that ADPANEL is based on an inviscid potential theory (hence, it is not able to directly model the boundary layer) numerical results reported in Figure 7 appear to be very good compared to the DPIV data obtained by Leishman. In such figure velocity profiles (normalized by the induced vertical velocity  $v$  from momentum theory) are depicted at two radial stations, namely  $r/R=0.8$  and  $r/R=1.0$ , and for two values of rotor height,  $z/R=1.0$  and  $z/R=1.5$ . Scatter points represent the experimental data, while numerical results are in solid lines. Only some deviations with respect to measurements were found to occur in the region closer to the ground, where viscous effects can not be neglected,

and where the interaction with boundary layer cannot be reproduced by an inviscid method.

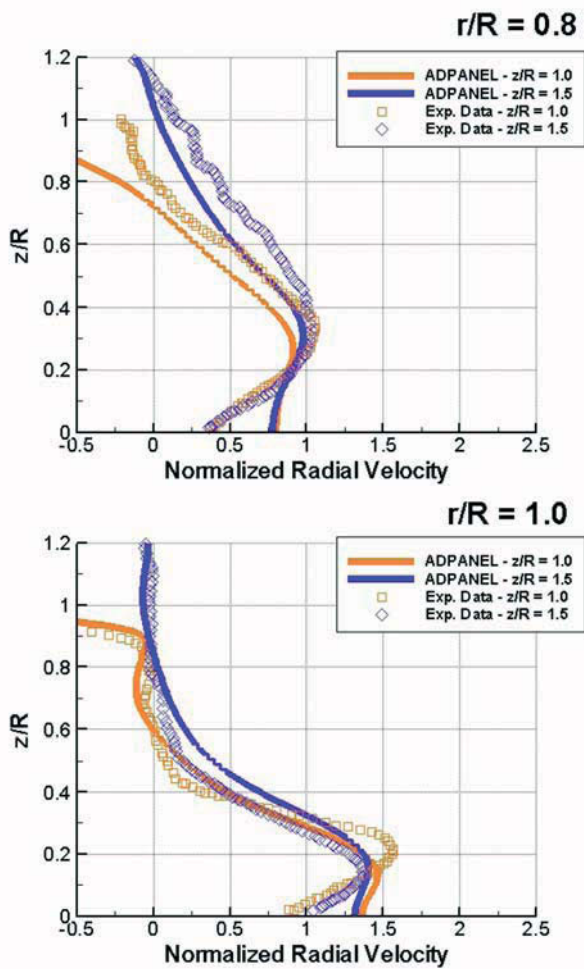


Figure 7: comparison between ADPANEL results and experimental measurements in terms of time-averaged velocity profiles.

Moreover, observing the flow visualizations reported in the same work, it is evident the difficulty to capture the dynamic evolution of vorticity in HIGE for whatever numerical tool.

In fact the flow is highly unsteady and characterized by important fluctuations around the averaged value, as shown in Figure 8. In this picture, the unsteady normalized radial velocity profiles are depicted every 60° of azimuth for the two radial stations considered before ( $r/R=0.8$  and  $r/R=1.0$ ) but for a fixed rotor height above the ground ( $h/R=1.0$ ). The time average is also reported in black to highlight the magnitude of the fluctuation.

From this study, we can conclude that ADPANEL is totally able to detect well both steady and unsteady velocity profiles generated by a rotor operating on ground (HIGE), correlating quite well with experimental data.

## 5 DESCRIPTION OF NUMERICAL SETUP

The geometrical characteristics of the rotor configuration adopted in this work are described in the following section. Then, the details of the conditions simulated and the procedure followed in the analysis are specified.

## 5.1 Baseline Helicopter Configuration

The rotorcraft configuration analyzed in the present work is a single main rotor helicopter. No fuselage and no tail rotor are taken into account in the following simulations. The four blades of the rotor are designed considering a simple rectangular planform and a constant 12% thickness cambered airfoil section. The total twist is 10° using a linear spanwise distribution. Two sets of blades, with solidity of  $\sigma=0.08$  and  $\sigma=0.12$  respectively, have been obtained by varying the blade chord. Rotor radius was set equal to unity in view of a non-dimensional treatment of the problem and the shaft axis is assumed to be perfectly vertical in order to simplify the analysis. The blades have been represented using 60-chordwise and 25-spanwise panels, with size refinements at the tip and at the leading and trailing edges. The rotor angular velocity is chosen in order to obtain a tip mach number of 0.6 in ISA SL conditions. The above described characteristics are in line with most conventional helicopters.

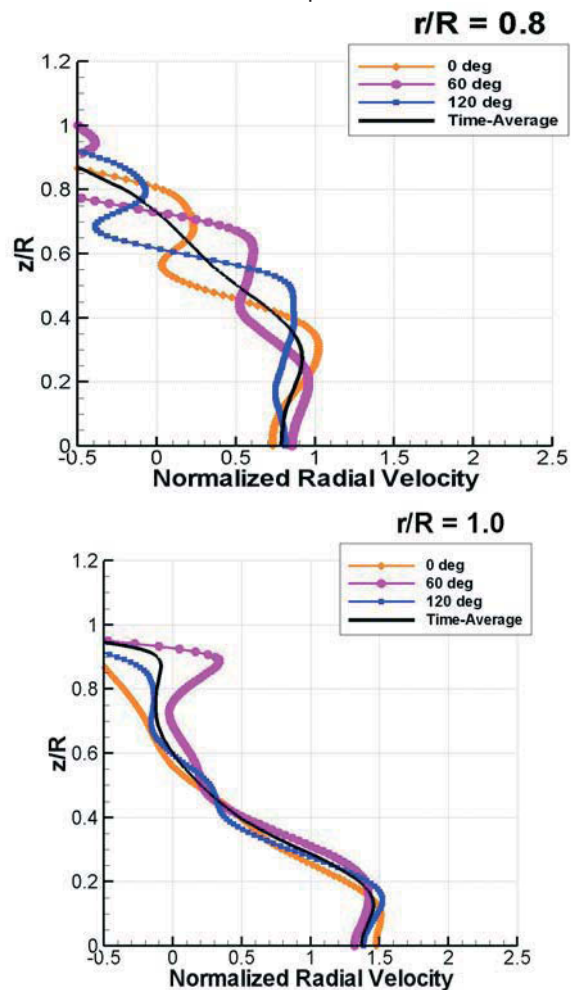


Figure 8. ADPANEL normalized radial velocity profile unsteadiness along last half revolution.

## 5.2 Description of Analyzed Conditions

The operating height of the helicopter was fixed at  $h/R=1$  for all the analyzed conditions. The operation at a constant disk- ( $C_T$ ) and blade-loading ( $C_T/\sigma$ ) between the two

sets of blades has been analyzed. At first, the effect of solidity was studied by trimming the two rotors at  $C_T=0.008$ . In this case, the rotor with  $\sigma=0.08$  was operated at  $C_T/\sigma=0.1$  (in the following named *case A*), while the one with  $\sigma=0.12$  at  $C_T/\sigma=0.066$  (*case B*). A second set of computations was carried out trimming the  $\sigma=0.12$  rotor at  $C_T/\sigma=0.1$  (*case C*), so that the two rotors' behaviors can be compared at the same value of blade loading, that is the one at which most of the helicopters fly. Next, for all the computations, the increase of the aircraft speed over the ground is simulated changing the freestream velocity, without any boundary condition on the ground apart from the symmetry (normal velocity component equals zero).

Considering the two sets of blades and the two trims, the same values of the normalized advance ratio  $\mu^*$  are considered in this study and are reported in Table 1 and Table 2. The normalized advance ratio is a measure of the backward deflection of the wake and is obtained by an approximation of the deflection angle as the ratio of the flight speed and the momentum theory induced velocity.

Condition N.	$V$ [m/s]	$V$ [kts]	$\mu$	$\mu^*$
1	0.00	0.00	0.000	<b>0.00</b>
2	5.20	10.11	0.025	<b>0.40</b>
3	6.50	12.63	0.032	<b>0.50</b>
4	7.80	15.16	0.038	<b>0.60</b>
5	9.00	17.49	0.044	<b>0.70</b>
6	10.30	20.02	0.050	<b>0.80</b>
7	11.60	22.55	0.057	<b>0.90</b>

**Table 1: operative conditions for the  $\sigma=0.08$  and  $\sigma=0.12$  rotors at  $C_T=0.008$ .**

Condition N.	$V$ [m/s]	$V$ [kts]	$\mu$	$\mu^*$
1	0.00	0.00	0.000	<b>0.00</b>
2	6.25	12.15	0.031	<b>0.40</b>
3	7.90	15.36	0.039	<b>0.50</b>
4	9.50	18.47	0.047	<b>0.60</b>
5	11.00	21.39	0.054	<b>0.70</b>
6	12.60	24.50	0.062	<b>0.80</b>
7	14.20	27.60	0.070	<b>0.90</b>

**Table 2: operative conditions for the  $\sigma=0.12$  rotor only at  $C_T=0.012$ .**

ADPANEL rotorcraft IGE calculations presented in the following are carried out considering one-hundred rotor revolutions at 10 degrees of azimuth step, in order to get accurate predictions of both radial and swirl velocities in proximity of the ground. In all results presented in this paper, it was made use of a vortex-image-system to represent the land.

## 6 NUMERICAL RESULTS

Numerical results presented in the following are divided in a first section that deals with the topological analysis of the flow around the rotor and in a second one that focuses on the unsteady fluctuations of the flowfield.

### 6.1 Flow Topology Description

Following the procedure described in the previous section, the HIGE condition is analyzed, comparing results at the same disk loading at first, and at the same blade loading next. Concerning the vortex wake structure behavior in HIGE conditions, several factors have to be taken into account. The vortices undergo two counteracting phenomena, whose effects depend on the rotor height from the ground: the viscosity and turbulent diffusion dominate at the higher heights while at lower ones, important stretching effects tend to oppose their resistance to normal diffusion. The interaction with the boundary layer, not modeled in ADPANEL, further complicates the overall fluid-dynamic field.

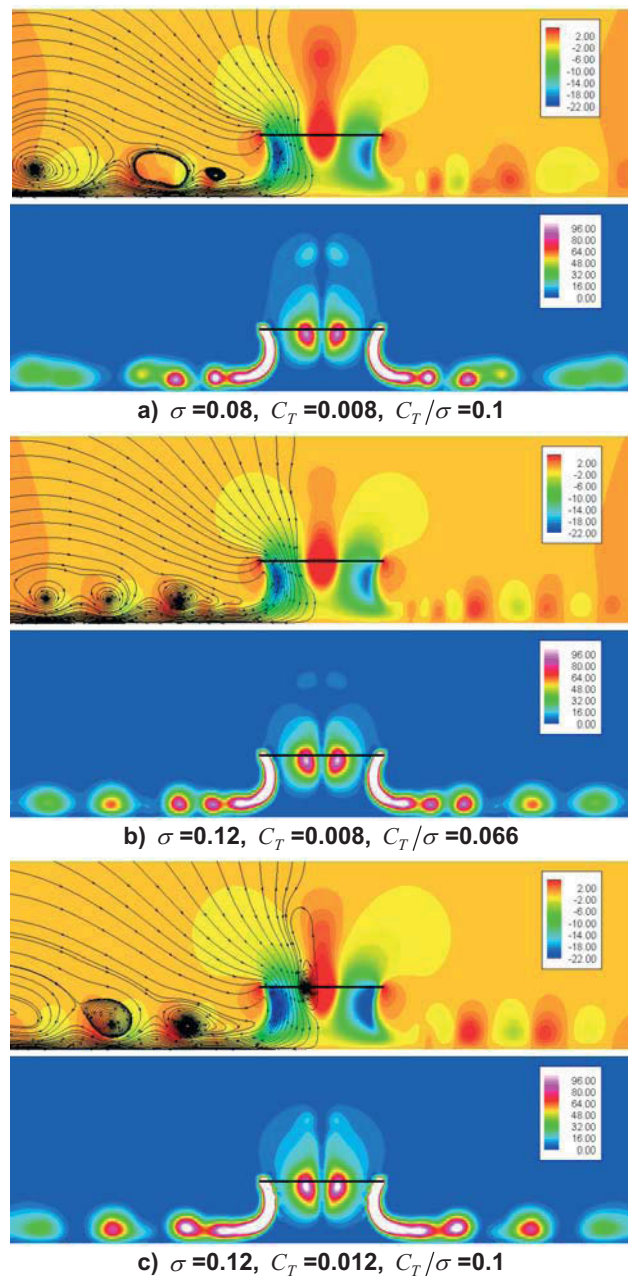


**Figure 9: snapshot of vertical velocity component (top, [m/s]) and magnitude of vorticity (bottom, [1/s]) after 100 rotor revolutions for the analysed cases.**

Observing the results obtained in HIGE shown in Figure 9 in terms of vertical velocity component and vorticity magnitude, some considerations can be drawn. First of all, the flow pattern for all the conditions analyzed is very similar (case A, B and C), and agrees with the expectation of a stagnation region beneath the rotor, the generation of a strong flow radial acceleration on the ground, and a wall jet development with significantly turbulent shear flow as the distance from the rotor increases. Considering the  $\sigma=0.12$  rotor at a higher blade loading (case C), the downwash is obviously increased, but the flow topology remains unchanged. The phenomenon itself is highly unsteady for all the conditions analyzed; in particular pairing and merging of the blade tip vortices occurs just near the ground, further increasing the unsteadiness of radial and swirl velocities.

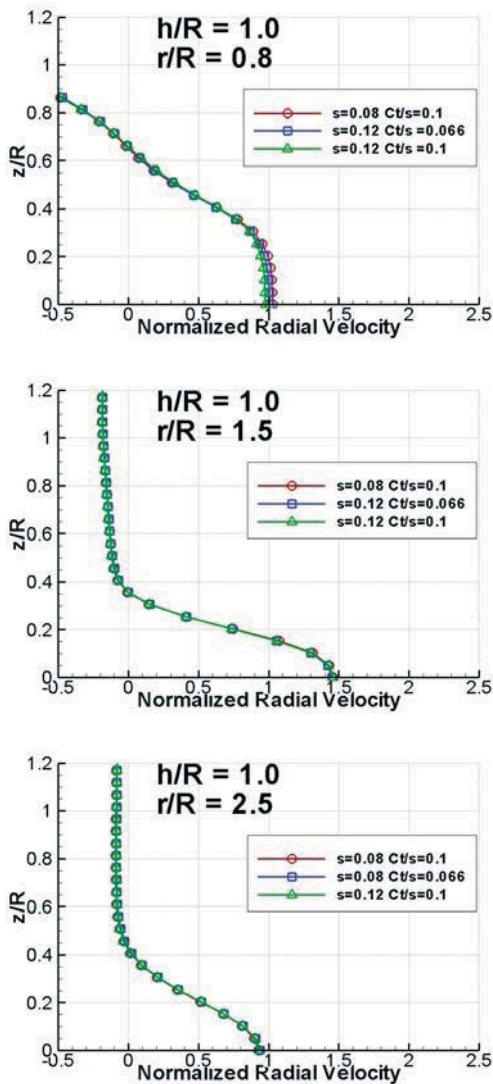


Figure 10: normalized radial velocity contour averaged over the last 40 rotor revolutions at  $h/R=1.0$  and radial stations  $r/R=0.8, 1.5, 2.5$ .

Radial velocity profiles (normalized by  $v$ ) showed in Figure 10 confirm the expected trend of the radial velocity close to the ground. From the stagnation region just below the disk, the flow strongly accelerates moving radially away from the rotor, and then decelerates for further

increase of radial distance due to the dissipation of the vortex structures.

Moreover, it can be noticed how the effect of solidity is negligible at all stations considered. Notice that, even if the radial velocity is stronger in case C, also the induced velocity is increased since the rotor thrust is higher. The two effects balance each other and the normalized velocity profiles are identical to cases A and B. Such behavior can be directly related to the intensity of the tip vortices  $\Gamma_v$ , trailed from each rotor blades and impinging on the ground. Such strength can be approximated as:

$$(4) \quad \Gamma_v = k\omega Rc \frac{C_T}{\sigma}$$

where from vortex theory the factor  $k=2$  can be assumed in hover, although was empirically found to be around  $k=2.3$ .

Tip speed, blade chord and loading are the governing parameters in the previous formula; but substituting in Eq. (4) the definition of solidity, the net circulation of the vortices impinging on the ground for a  $n$ -bladed rotor is:

$$(5) \quad n\Gamma_v = k\omega\pi R^2 C_T$$

Notice that the total strength of the wake depends only on angular velocity, disk area and disk loading, independently on the value assumed by rotor solidity. All these parameters are the same in cases A and B presented up to now, implying an analogous wake development. In case C, as explained, the thrust is higher, so the vortices will be also stronger with a consequent higher radial velocity, but with the same non-dimensional profiles.

Increasing the advance ratio from the HIGE regime, the freestream opposes to the radial pattern of the vortices upwind of the rotor. Then, the vortices begin to pair and merge together, initially far away from the rotor axis.

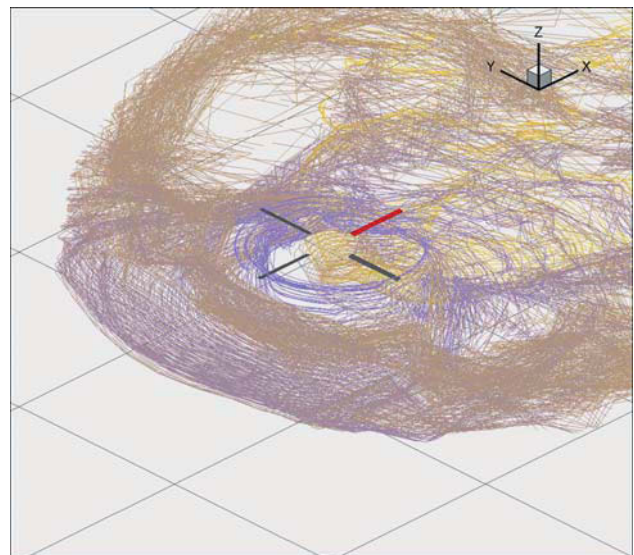


Figure 11: example of wake development for case A rotor at  $\mu^*=0.60$ .

Considering the three cases simulated (A, B and C), at a normalized advance ratio of  $\mu^*=0.40-0.50$ , the vortices form a clear unsteady recirculation pattern that affect the forward part of the rotor disk. Two stagnation points, separated by a reverse flow region (*recirculation zone*),

are present on the ground. The unsteady fluctuations are still moderate and the stagnation points oscillation in space is not significant. The full development of the recirculation regime occurs at  $\mu^* = 0.6$  (Figure 11), when the vortical pattern enlarges and places just in correspondence of the rotor disk tip. Velocity oscillations are significantly higher. Considering an higher forward speed ( $\mu^* = 0.70$  - Figure 12), a well defined ground vortex forms as soon as the recirculation passes under the rotor disk leading edge. The area just in front of the rotor is now more uniform.

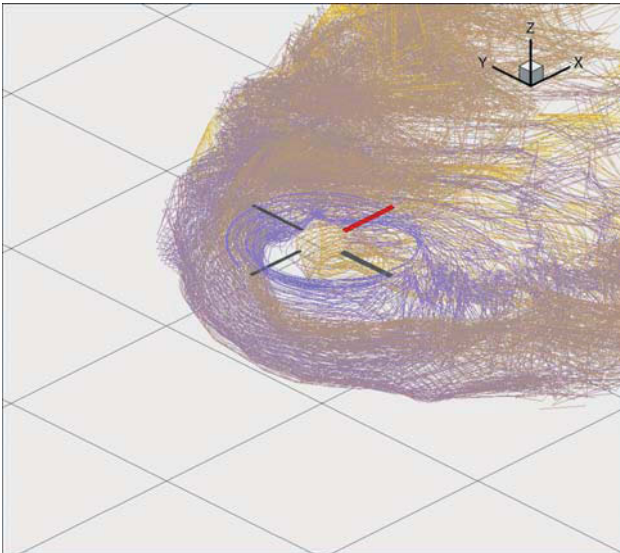


Figure 12: example of wake development for case A rotor at  $\mu^* = 0.70$ .

The ground vortex state is still present at  $\mu^* = 0.80$  (Figure 13), but for further increase in speed it is overrun by the freestream (sometimes intermittently in time), and the flow is more similar to OGE operation ( $\mu^* = 0.90$  - Figure 14).

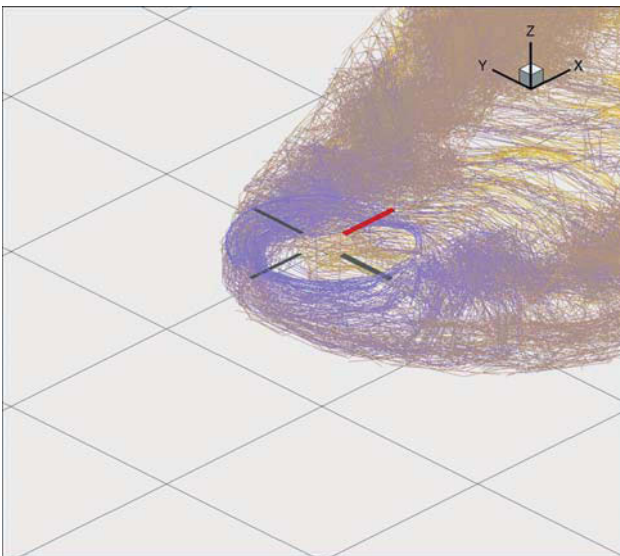


Figure 13: example of wake development for case A rotor at  $\mu^* = 0.80$ .

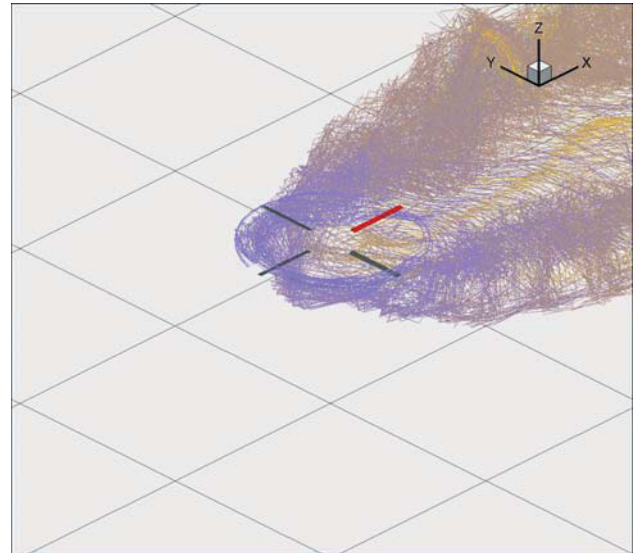


Figure 14: example of wake development for case A rotor at  $\mu^* = 0.90$ .

In all the aforementioned conditions, the flowfield is always very similar, confirming the conclusions found in HIGE by means of the tip vortex model that the behavior does not depend on  $\sigma$  even at different blade loadings, assuming to work at the same  $\mu^*$  value. In fact, in case C, the higher velocity on ground does not modify the flowfield because the freestream velocity is also stronger. Changing the point of view, from a pilot perspective, both case A and B will encounter the same aerodynamic regime of case C at lower speed.

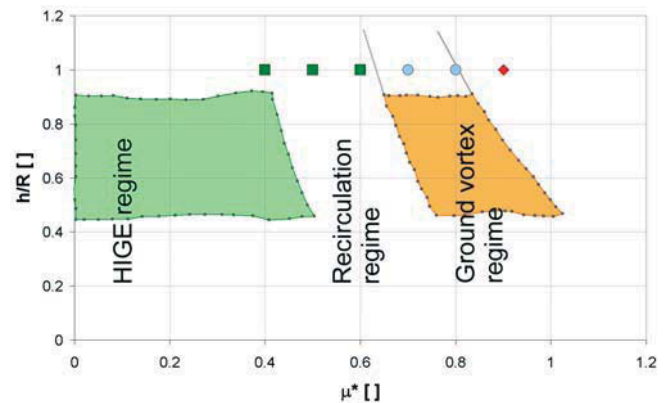


Figure 15: summary of the numerical computations: green boxes represents recirculation regime, blue circles the ground vortex state and red diamonds the final vortex overrunning in the case of  $C_T = 0.008$ . Experimental boundaries come from Curtiss et al.<sup>[13]</sup>.

In Figure 15 we reported the experimental boundaries tracked in the original document of Curtiss et al.<sup>[13]</sup> which clearly defined the occurring of two different regimes (recirculation and ground vortex) with the increasing of normalized advance ratio  $\mu^*$  (for the same value of  $h/R$ ).

In this pioneer work, such boundaries were determined by means of flow visualizations, yielding to the conclusion

that both rotor height, and normalized advance ratio  $\mu^*$ , are the main parameters governing the transition between different regimes. In the same figure, the numerical results are summarized taking into account the flow visualization reported in Figure 16, Figure 17 and Figure 20.

Recirculation regimes were numerically found to occur for  $\mu^* = 0.40, 0.50$  and  $0.60$  as can be observed in subfigures a). These ones are reported in Figure 15 by means of green boxes. A clearly formed ground vortex was observed to be born under the leading edge of rotor disk for an advance ratio of  $\mu^* = 0.70$  (subfigures b)). Ground vortex dominated regimes, indicated by blue circles, extended in computations up to the theoretical limit, that is  $\mu^* = 0.80$ , where the vortex structure lying on ground has lost the major part of its intensity and can disappear intermittently, as found in cases B and C (subfigures c)). Finally, considering higher advance ratio, a numerical computation was carried out at  $\mu^* = 0.90$  (red diamond), confirming the tendency of the rotor wake structure to come back very similar to the OGE one for high aircraft velocities (subfigures d)).

The first partial conclusion that arises from the above comparison is that ADPANEL agrees very well with the Curtiss et al. analysis concerning the identification of the flow regimes.

The effect of a different solidity is, as expected, limited to some details of the flowfield, but does not affect the flight regimes, as fully demonstrated by presented numerical computations. The effect of an higher disk loading is, as explained, balanced by the increase in the freestream required to maintain the same normalized advance ratio. More in detail, observing Figure 16, Figure 17 and Figure 20, it can be stated that the recirculation pattern tends to be formed a bit more upstream in case of higher solidity. Moreover, once the ground vortex state is reached, it evolves quickly than for a low solidity rotor. Such assertion is even supported by assessing the averaged stagnation points position, as the forward speed increases. Figure 18 shows that such position shifts aft with the increase of  $\mu^*$ . However, the movement is not the same for the two values of solidity considered, but shows some marginal differences.

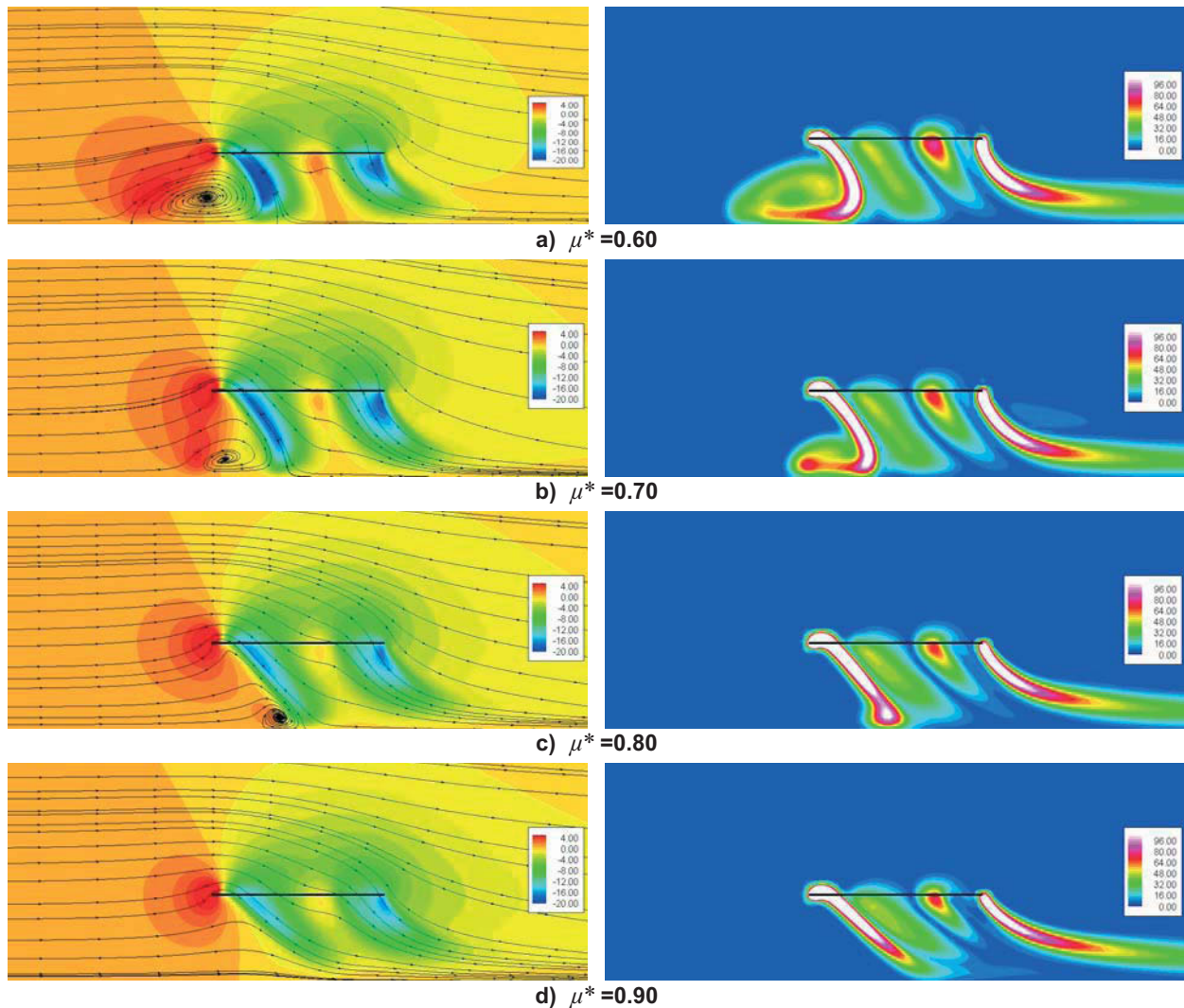


Figure 16: vertical velocity contour (left, [m/s]) and magnitude of vorticity (right, [1/s]) averaged over the last 40 rotor revolutions for  $\sigma = 0.08$  at  $C_T = 0.008$  – side view.

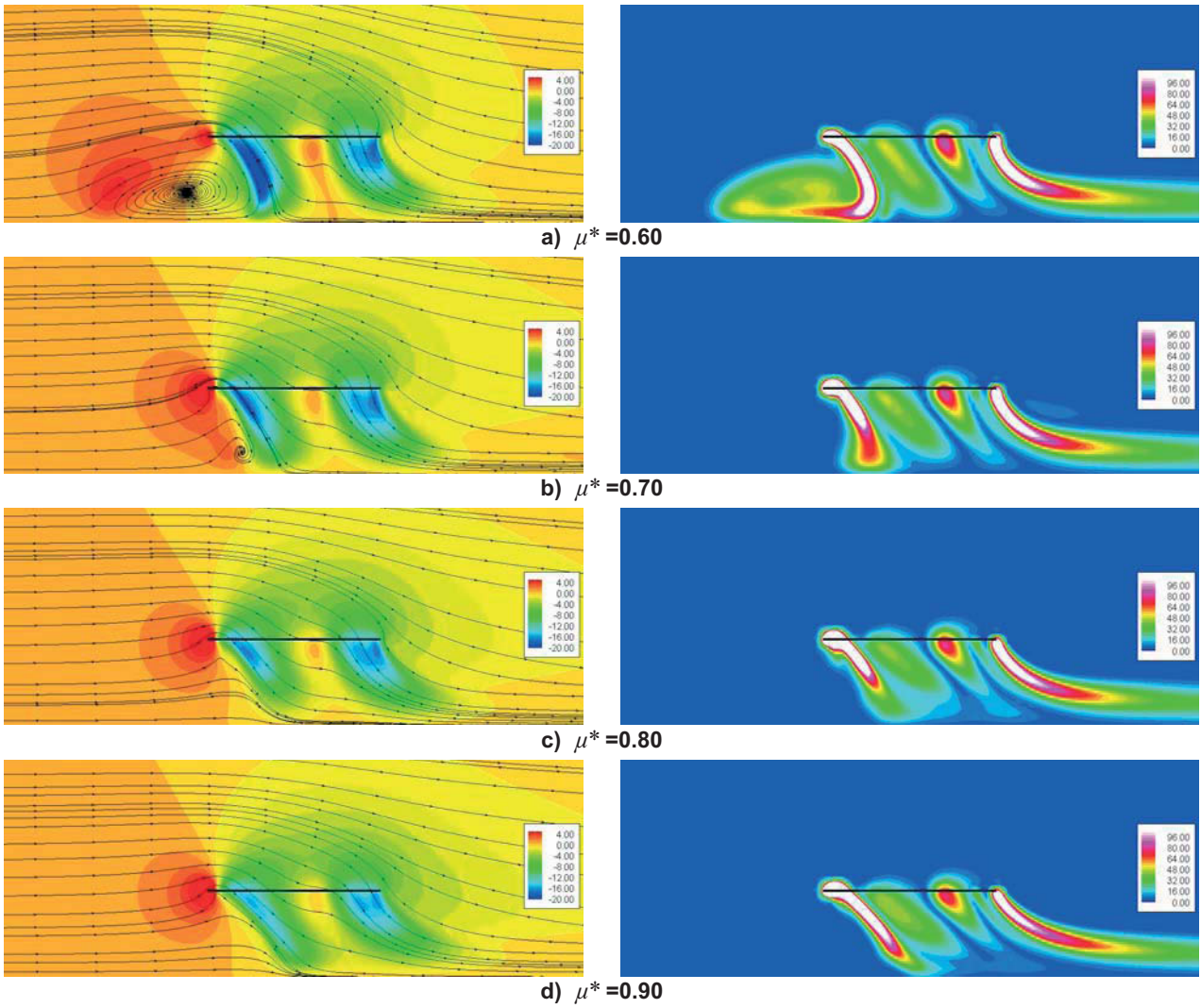


Figure 17: vertical velocity contour (left, [m/s]) and magnitude of vorticity (right, [1/s]) averaged over the last 40 rotor revolutions for  $\sigma = 0.12$  at  $C_T = 0.008$  – side view.

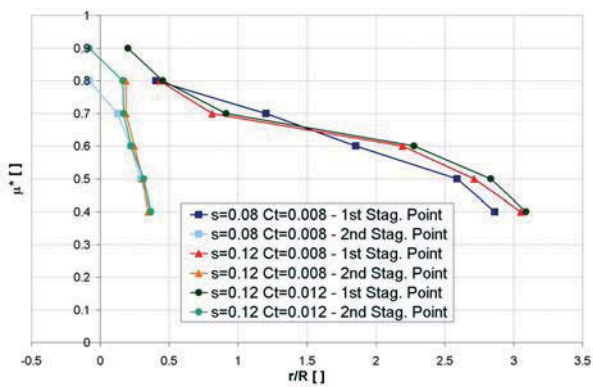


Figure 18: averaged stagnation points position.

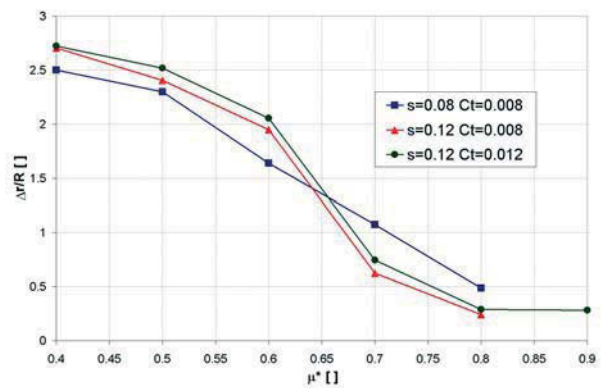


Figure 19: averaged vortex dimension computed as distance between the averaged stagnation points.

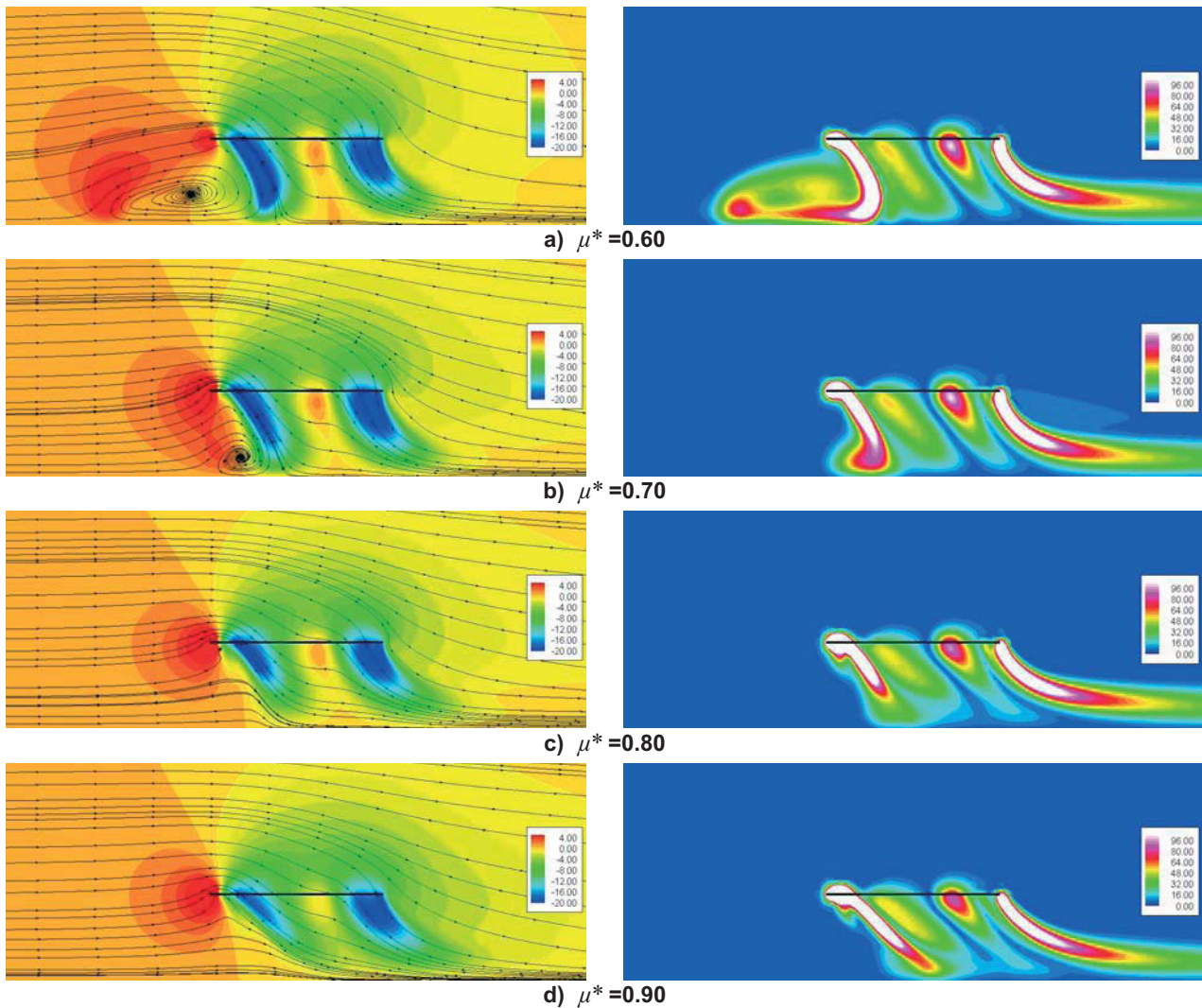


Figure 20: vertical velocity contour (left, [m/s]) and magnitude of vorticity (right, [1/s]) averaged over the last 40 rotor revolutions for  $\sigma=0.12$  at  $C_T=0.012$  – side view.

## 6.2 Flow Unsteadiness Assessment

From the topological analysis of the aerodynamic environment, the need for a suitable post-processing able to highlight the flow unsteadiness is made evident. For this purpose, the root mean square has been applied to the deviation of the in-plane velocity and to the vorticity. Such RMS deviations are computed over the last 40 rotor revolutions.

Figure 21, Figure 22 and Figure 23 report the RMS of the in-plane velocity component and of the normalized RMS (on the average value) of the vorticity magnitude on the longitudinal planes through the rotor hub center for the forward flight conditions previously analyzed. This last entity represents the percentage oscillation of vorticity, allowing to identify vortices intermittency. High values of unsteadiness are associated to the red color.

An accurate analysis reveals the formation of the recirculation region in front of the rotor, with an increasing level of unsteadiness as long as it approaches the rotor

disk, before passing in ground vortex regime. At  $\mu^*=0.60$  the fluctuations in correspondence of the stagnation point manifest themselves for both values of solidity, but showing as expected an increasing with the disk loading value (case C).

Considering higher normalized advance ratios, the ground vortex generation and its consequent overrunning can be observed. The effect of solidity in these conditions is relevant only below the forward part of the disk, while the increasing in  $C_T$  affects even the wake development behind the rotor.

Moreover, previous pictures confirm the intermittent ground vortex onset at  $\mu^*=0.80-0.90$ , already highlighted by the study of the stagnation points. The same considerations regarding the effect of solidity as the normalized advance ratio increase are supported even by the RMS analysis on the lateral plane, not reported in this work.

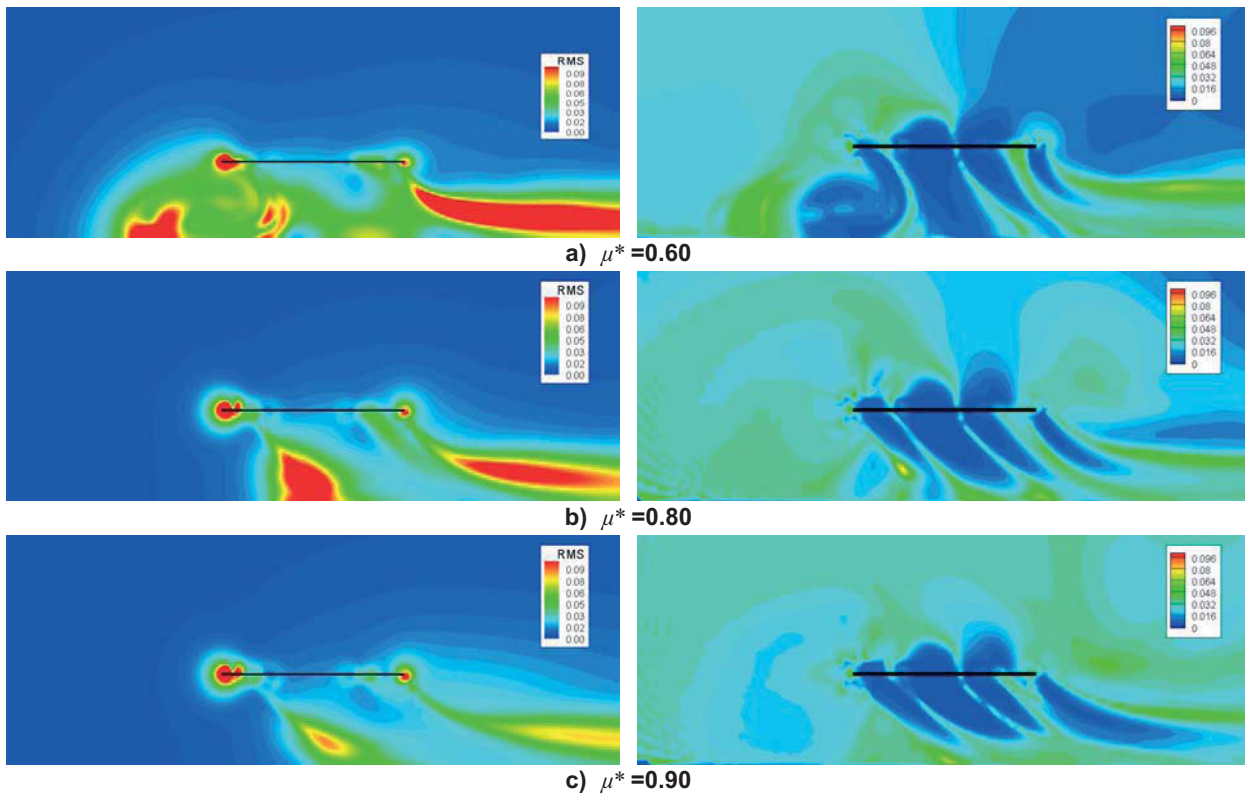


Figure 21: contour of the RMS over the last 40 rotor revolutions of the in-plane velocity (left, [m/s]) and of the RMS of vorticity magnitude normalized on the average value for  $\sigma = 0.08$  at  $C_T = 0.008$  – side view.

## 7 CONCLUSIONS

Aim of this paper was the investigation of the aerodynamic behavior of a rotor operating in ground effect using the AgustaWestland in-house developed tool ADPANEL, which basic features have been reported at the beginning of this work.

The numerical method presented here was fully validated in HIGE conditions, taking into account the exhaustive and remarkable experimental work recently reported by Leishman et al., showing a good agreement both in terms of performances and of velocity profiles. Subsequently, present tool was directly applied to both hovering and forward flight IGE conditions, taking into account different rotor configurations by combining different values of solidities and disk-loadings and main results reported in the course of this work.

Self-similarity of averaged-normalized-velocity profiles on ground was observed in HIGE for all the conditions analyzed in this paper, since the stronger outwash due to higher thrust value was balanced by the consequent higher induced velocity. According to experimental evidence, ADPANEL results in HIGE clearly showed the existence of strong flowfield unsteadiness and the generation of important vortical structures along the ground moving far away from the rotor.

Numerical computations showed the capabilities of present tool to recognize all different flow-regimes that normally characterize rotor operations in slow-speed

forward flight IGE conditions. By means of velocity and vorticity analysis, the generation of the '*recirculation regime*' was successfully predicted by numerical results. The evolution to the subsequent '*ground vortex regime*', and its final overrunning, was observed in the computations too, showing an excellent agreement with the experimental diagram by Curtis et al..

Numerical results showed that assuming to work at the same normalized advance ratio (even for different values of rotor solidity, or for different values of rotor disk-loadings), the flowfield topology is not significantly altered. For example, in case of higher disk-loadings, freestream and radial outwash velocity both increase and counter-balance themselves, further confirming experimental observations by Curtiss et al.. Hence, the same aerodynamic regime will be encountered at lower speeds by rotors operating at lower disk loadings.

The effect of solidity at constant disk- or blade-loadings, is limited to some details of flowfield topology, but does not affect significantly the regime onset and its temporal evolution.

Finally, flowfield unsteadiness was assessed for the conditions analyzed in this work, by means of a RMS post-processing. Numerical results showed an increasing of intermittency in the recirculation region, as long as it approaches the rotor with the increasing of forward flight speed.

Velocity and vorticity unsteadiness was found to be very strong in the vortex structure below the rotor disk in ground vortex regime as well.

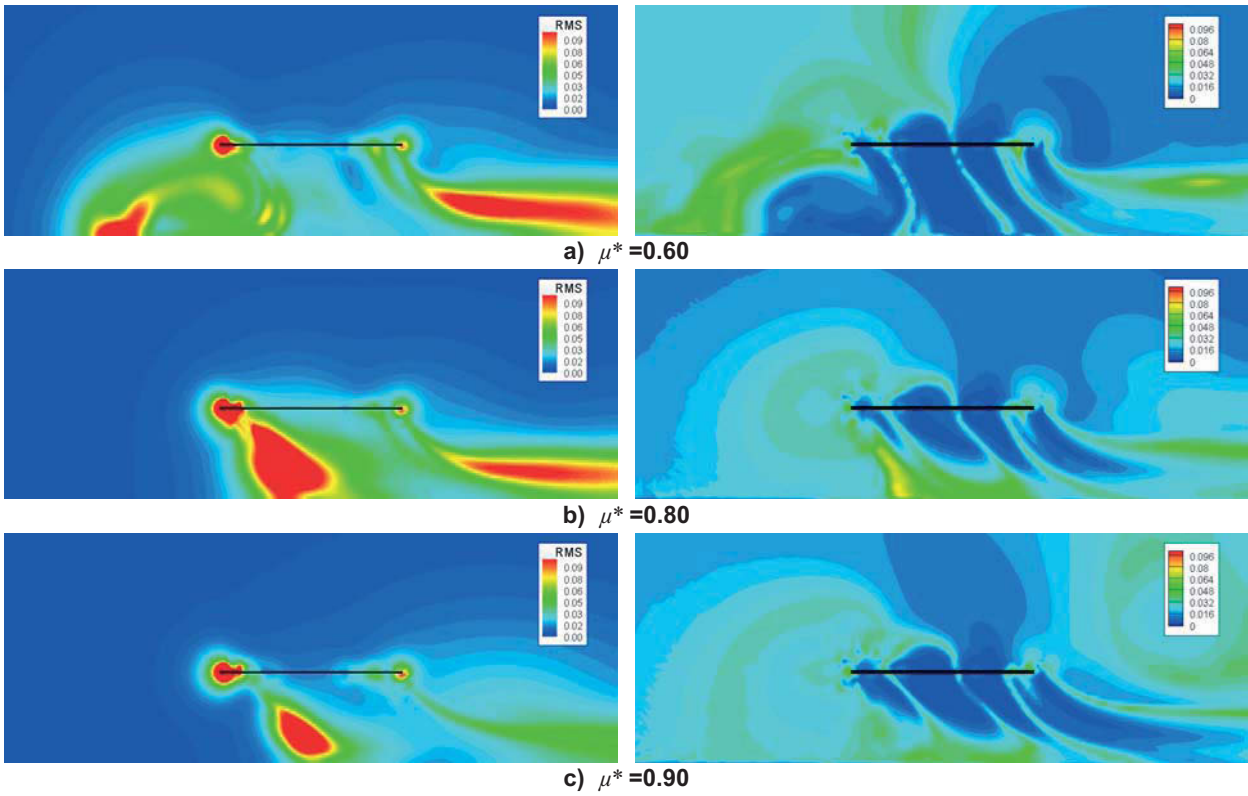


Figure 22: contour of the RMS over the last 40 rotor revolutions of the in-plane velocity (left, [m/s]) and of the RMS of vorticity magnitude normalized on the average value for  $\sigma = 0.12$  at  $C_T = 0.008$  – side view.

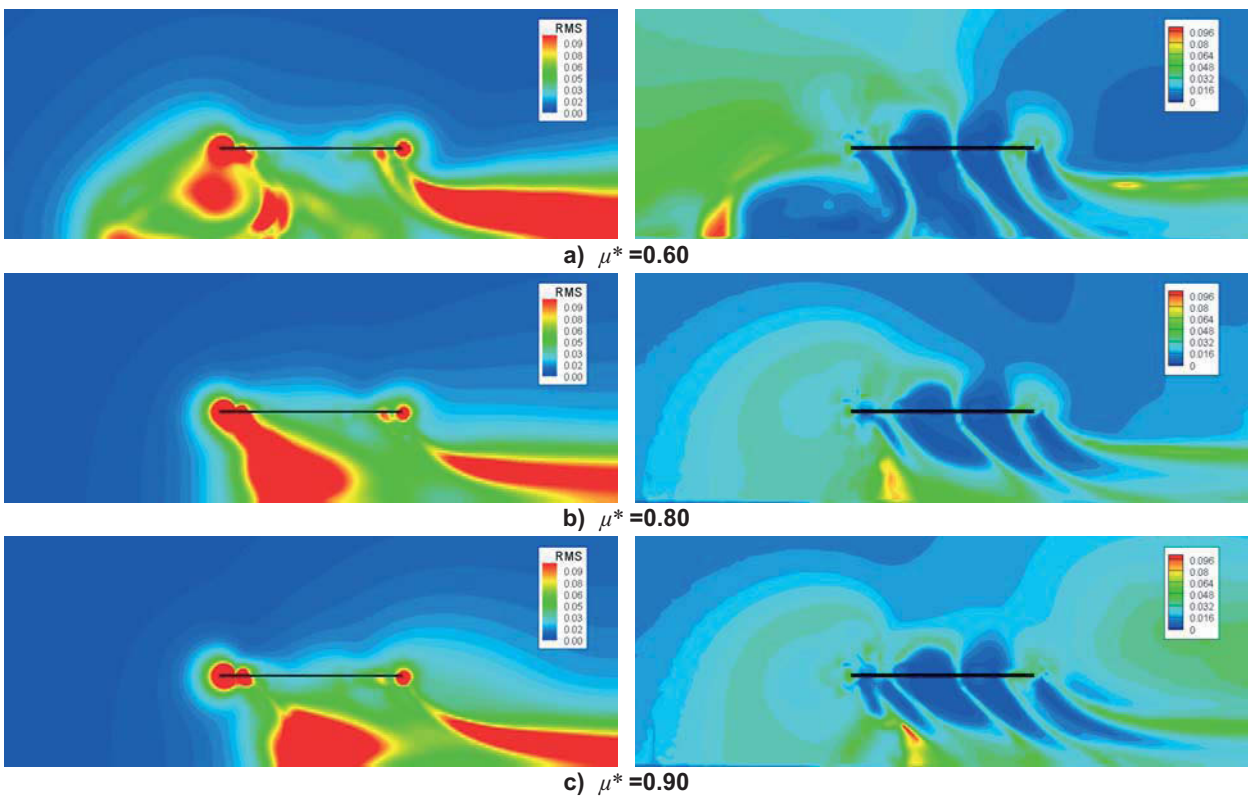


Figure 23: contour of the RMS over the last 40 rotor revolutions of the in-plane velocity (left, [m/s]) and of the RMS of vorticity magnitude normalized on the average value for  $\sigma = 0.12$  at  $C_T = 0.012$  – side view.

## 8 REFERENCES

- [1] Wachspress, D.A., Quackenbush, T.R., Boschitsch, A.H., "First-Principles Free-Vortex Wake Analysis for Helicopter and Tiltrotors", 59<sup>th</sup> American Helicopter Society Annual Forum, Phoenix, AZ, May 6-8, 2003.
- [2] Wachspress, D.A., Quackenbush, T.R., Boschitsch, A.H., "Rotor Interactional Aerodynamics Calculation with Fast Vortex/Fast Panel Methods", 56<sup>th</sup> American Helicopter Society Annual Forum, Virginia Beach, VA, May 2-4, 2000.
- [3] D'Andrea, A., "Development of a Multi-Processor Unstructured Panel Code Coupled with a CVC Free Wake Model for Advanced Analyses of Rotorcrafts and Tiltrotors", 64<sup>th</sup> American Helicopter Society Annual Forum, Montreal, Canada, April 29 – May 1, 2008.
- [4] Bagai, A., Leishman, J.G., "Free-Vortex Filament Methods for the Analysis of Helicopter Rotor Wakes", Journal of Aircraft, Vol. 39, N. 5, Sept-Oct 2002.
- [5] D'Andrea, A., Scandroglio, A., Melone, S., "Numerical Analysis of Advanced-Innovative Tiltrotor Configurations", 34<sup>th</sup> European Rotorcraft Forum, Liverpool, UK, September 16-19, 2008.
- [6] Ramasamy, M., Leishman, J.G., "Reynolds Number Based Blade Tip Vortex Model", 61<sup>st</sup> American Helicopter Society Annual Forum, Grapevine, TX, June, 2005.
- [7] Bhagwat, M.J., Leishman, J.G., "Generalized Viscous Vortex Model for Application to Free-Vortex Wake and Aeroacoustic Calculation", 58<sup>th</sup> American Helicopter Society Annual Forum, Montreal, Canada, June, 2002.
- [8] Greengard, L., Rokhlin, V., "A Fast Algorithm for Particle Simulations", Journal of Computational Physics, 73, 325-348, 1987.
- [9] Greengard, L., Rokhlin, V., "On the Efficient Implementation of the Fast Multiple Algorithm", Department of Computer Science Research Report 602, Yale University, 1988.
- [10] Leishman, J. G., Ramasamy, M., Lee, T. E., "Fluid Dynamics of Interacting Blade Tip Vortices with a Ground Plane", 64<sup>th</sup> American Helicopter Society Annual Forum, Montreal, Canada, April 29 – May 1, 2008.
- [11] Ganesh, B., Komerath, N., "Unsteady Aerodynamics of Rotorcraft in Ground Effect", AIAA Paper 2004-2431, Fluid Dynamics Meeting, Portland, OR, June, 2004.
- [12] Saijo, T., Ganesh, B., Huang, A., Komerath, N., "Development of unsteadiness in a rotor wake in ground effect", 21<sup>st</sup> Applied Aerodynamics Conference, Orlando, FL, June 23-26, 2003.
- [13] Curtiss, H. C., Sun, M., Putman, W. F., Hanker, E. J., "Rotor Aerodynamics in Ground Effect at low advance ratios", 37<sup>th</sup> American Helicopter Society Annual Forum, New Orleans, LA, May, 1981.
- [14] Curtiss, H. C., Erdman, W., Sun, M., "Ground effect Aerodynamics", Vertica, Vol. 11, No 1/2, pagg. 29-42, 1987.
- [15] D'Andrea, A., "Numerical Analysis of Unsteady Vortical flows Generated by a Rotorcraft Operating on Ground: a First Assessment of Helicopter Brownout", 65<sup>th</sup> American Helicopter Society Annual Forum, Grapevine, TX, May 27-29, 2009.
- [16] Pahlke, K., Chelli, E., "Calculation of Multi-bladed Rotors in Forward Flight Using a3D Navier-Stokes Method", proc. 26<sup>th</sup> European Rotorcraft Forum, The Hague, Netherlands, Paper N.48, 2000.
- [17] Decours, J., Lefebvre, T., "Navier-Stokes Computations Applied to Tilt-rotors", 33<sup>rd</sup> European Rotorcraft Forum, Kazan, Russia, September 11-13, 2007.
- [18] Phillips, C., Brown, R. E., "Eulerian Simulation of the Fluid Dynamics of Helicopter Brownout", 64<sup>th</sup> American Helicopter Society Annual Forum, Montreal, Canada, April 29-May 1, 2008.
- [19] Fradenburgh, E. A., "Aerodynamic Factors Influencing Overall Hover Performance", AGARD-CP-111, 1972.
- [20] Fradenburgh, E. A., "The Helicopter and the Ground Effect Machine", Journal of the American Helicopter Society, Vol. 5(4), pp. 26-28, 1960.
- [21] Cheeseman, I. C., Bennet, W. E., "The Effect of the Ground on a Helicopter Rotor in Forward Flight", Tech. Report ARC R&M 3012, Aeronautical Research Council, 1957.
- [22] Katz, J., Plotkin, A., "Low-speed Aerodynamics. From Wing Theory to Panel Methods", McGraw-Hill Series in Aeronautical and Aerospace Engineering, 1991